

1  
2  
3  
4  
5  
6  
7  
8  
9  
10  
11  
12  
13  
14  
15  
16  
17  
18  
19  
20  
21  
22

# Applicability Domain of Polyparameter Linear Free Energy Relationship Models Evaluated by Leverage and Prediction Interval Calculation

*Satoshi Endo<sup>1,2</sup>*

<sup>1</sup> Health and Environmental Risk Division, National Institute for Environmental Studies (NIES), Onogawa 16-2, 305-8506 Tsukuba, Ibaraki, Japan

<sup>2</sup> Graduate School of Engineering, Osaka City University, Sugimoto 3-3-138, Sumiyoshi, 558-8585 Osaka, Japan

Contact information:

Satoshi Endo

Health and Environmental Risk Division

National Institute for Environmental Studies (NIES)

Onogawa 16-2, 305-8506 Tsukuba, Ibaraki

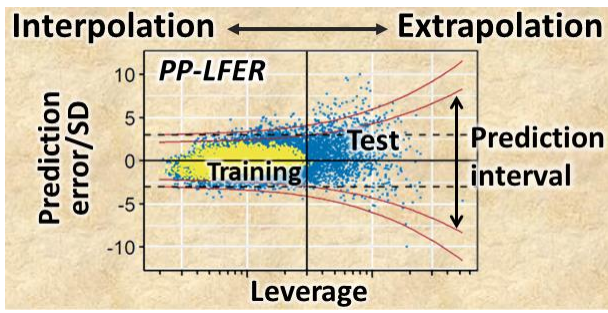
Japan

Phone: ++81-29-850-2695

Fax: ++81-29-850-2870

Email: endo.satoshi@nies.go.jp

23 TOC graphic



24

25

## 26 **Abstract**

27 Polyparameter linear free energy relationships (PP-LFERs) are accurate and robust models  
28 employed to predict equilibrium partition coefficients ( $K$ ) of organic chemicals. The accuracy  
29 of predictions by a PP-LFER depends on the composition of the respective calibration data set.  
30 Generally, extrapolation outside the model calibration domain is likely to be less accurate  
31 than interpolation. In this study, the applicability domain (AD) of PP-LFERs was systematically  
32 evaluated by calculating the leverage ( $h$ ) and prediction interval (PI). Repeated simulations  
33 with experimental data showed that the root mean squared error of predictions increased  
34 with  $h$ . However, the analysis also showed that PP-LFERs calibrated with a large number (e.g.,  
35 100) of training data were highly robust against extrapolation error. For such well-calibrated  
36 PP-LFERs, the common definition of extrapolation ( $h > 3 h_{\text{mean}}$ , where  $h_{\text{mean}}$  is the mean  $h$  of  
37 all training compounds) may be excessively strict. Alternatively, the PI is proposed as a metric  
38 to define the AD of PP-LFERs, as it provides a concrete estimate of the error range that agrees  
39 well with the observed errors, even for extreme extrapolations. Additionally, published PP-  
40 LFERs were evaluated in terms of their AD using the new concept of AD probes, which  
41 indicated the varying predictive performance of PP-LFERs in existing literature for  
42 environmentally relevant compounds.

43

## 44 **Keywords**

45 Applicability domain, linear solvation energy relationship, extrapolation, property prediction,  
46 partition coefficient, QSAR, QSPR, perfluoroalkyl substances

47

## 48 **Synopsis**

49 Calculating the prediction intervals delineates the applicability domain of polyparameter  
50 linear free energy relationship models.

51

52

## 53 1. Introduction

54 Equilibrium partition coefficients largely determine the environmental distribution of organic  
55 contaminants and are crucial parameters for environmental risk assessments. Among various  
56 models, the linear solvation energy relationships (LSERs),<sup>1</sup> or generally, polyparameter linear  
57 free energy relationships (PP-LFERs) that use Abraham's solute descriptors have been  
58 confirmed to be accurate and robust for predicting partition coefficients.<sup>2</sup> The PP-LFERs cover  
59 the intermolecular interactions relevant to the phase partitioning of neutral organic  
60 compounds. Their successful environmental applications have been previously reviewed.<sup>3,4</sup>

61 PP-LFERs are multiple linear regression models that typically use five solute  
62 descriptors. The following three types of equations are most often applied.<sup>1,5</sup>

$$63 \quad \text{Log } K = c + eE + sS + aA + bB + vV \quad (1)$$

$$64 \quad \text{Log } K = c + eE + sS + aA + bB + lL \quad (2)$$

$$65 \quad \text{Log } K = c + sS + aA + bB + vV + lL \quad (3)$$

66 The symbols denote the following:  $K$ , partition coefficient;  $E$ , excess molar refraction;  $S$ , solute  
67 polarizability/dipolarity parameter;  $A$ , solute hydrogen (H)-bond donor property;  $B$ , solute H-  
68 bond acceptor property;  $V$ , McGowan's molar volume; and  $L$ , logarithmic hexadecane/air  
69 partition coefficient. The lowercase letters are regression coefficients and are typically trained  
70 with several tens of compounds for which experimental  $\log K$  and the solute descriptors (i.e.,  
71  $E$ ,  $S$ ,  $A$ ,  $B$ ,  $V$ , and  $L$ ) are available. The fitting of the PP-LFERs is high even to data that are highly  
72 diverse in size and polarity. For solvent/water and solvent/air partition coefficients, the  
73 calibration typically results in a standard deviation (SD) of 0.2 or below for the  $\log K$  values.<sup>1</sup>  
74 Partition systems that involve a heterogeneous phase (e.g., natural organic matter) can  
75 exhibit a lower quality of fit (SD, 0.3–0.5 log units).<sup>3</sup>

76 PP-LFERs are derived from a multiple linear regression; therefore, their applicability  
77 domain (AD) is related to the training (calibration) set of compounds. Generally, extrapolation  
78 (i.e., prediction beyond the calibrated domain) is likely to be less accurate than interpolation.  
79 Moreover, a long-range extrapolation is expected to be more error-prone than a short-range  
80 extrapolation. However, in a multidimensional space (here, 5 descriptors), it is unclear how  
81 the terms interpolation and extrapolation can be defined and how a quantitative relationship  
82 between the extent of extrapolation and prediction accuracy may be established. Notably, an  
83 extrapolation can be less accurate but is not necessarily inaccurate or unreliable. The required

84 accuracy depends on the purpose of the model use, and extrapolation can be acceptable  
85 within the range where its accuracy is satisfactory.

86 Among various approaches, calculation of the leverages has been considered to define  
87 and evaluate the AD for linear regression models.<sup>6-9</sup> The leverage is a quantitative measure of  
88 the distance from the entire set of calibration data. Leverage calculation is applied to identify  
89 outliers within the calibration set, and it can also be used to quantitatively define  
90 extrapolation in the prediction. A large leverage value indicates a long distance from the  
91 calibrated domain and thus an extrapolation with the possibility of increased error.

92 The prediction interval (PI) is the range of values where future model predictions are  
93 expected to fall at a given frequency. Typically, 95 or 99% PIs are calculated. Although PIs are  
94 frequently calculated for predictions by a simple linear regression model, they are not  
95 commonly presented for multiple linear regression models, including PP-LFERs. However, the  
96 PI can be more useful than the leverage, as the PI considers both the distance from the  
97 calibration set and the quality of the model fitting (see Section 2.2 for more details).

98 The purposes of this study are three-fold: (i) To quantitatively demonstrate how the  
99 prediction accuracy of a PP-LFER decreases when moving away from a specific domain of  
100 calibration defined by the leverage, (ii) to compare actual prediction errors with error margins  
101 expected by PIs, and (iii) to evaluate several calibration sets for PP-LFERs in terms of their AD  
102 using a new concept of AD probes. On the basis of these, a discussion is presented on the  
103 definition and evaluation of AD for PP-LFER models. The information should also be helpful  
104 for the future development of PP-LFERs because it ensures an optimized calibration data set.

105

## 106 **2. Methodology**

### 107 **2.1 Definition and calculation of the leverage and PI**

108 The definition and calculation of the leverage and PI are described in full in SI-1 of the  
109 Supporting Information (SI) and only briefly here.

110 The PP-LFER regression can be expressed in matrix form as follows,

$$111 \quad y = X \beta + \varepsilon \quad (4)$$

112 where  $y$  is the vector of observations for  $\log K$ ,  $\beta$  is the vector of regression coefficients, and  
113  $\varepsilon$  is the error vector.  $X$  is the design matrix containing solute descriptors of  $n$  training  
114 compounds. The hat matrix ( $H$ ) can be derived from  $X$ , and the diagonals of  $H$  (i.e.,  $h_{ii}$ ) are

115 referred to as the leverages and infer the distance of each calibration compound from the  
 116 others in terms of the solute descriptor combination.  $h_{ii}$  is between 0 and 1, and the sum of  
 117  $h_{ii}$  for the  $n$  training compounds is equal to the number of fitting parameters  $p$ , which is 6 for  
 118 the PP-LFERs (including the regression constant). An overly high  $h_{ii}$  indicates that the  
 119 respective calibration compound is an outlier in terms of its descriptors. Typically,  $h_{ii} = 3h_{\text{mean}}$   
 120 is considered a threshold value,<sup>6-9</sup> where  $h_{\text{mean}}$  is the mean of  $h_{ii}$  for all calibration compounds  
 121 and is equal to  $p/n$ . To evaluate the extrapolation for compound  $j$ , which is not included in  
 122 the calibration set,  $h$  is calculated as,

$$123 \quad h = x_j^T (X^T X)^{-1} x_j \quad (5)$$

124 where  $x_j$  is the column vector containing the solute descriptors of  $j$ . Analogous to the  
 125 identification of outliers in the training set,  $h = 3h_{\text{mean}}$  is typically considered the threshold  
 126 value for extrapolation.<sup>6-9</sup>

127 The PI of the PP-LFER can be expressed as  $[\log K_j - \Delta(\log K), \log K_j + \Delta(\log K)]$ , where  
 128  $\log K_j$  is the value for compound  $j$  predicted with eq 4 (i.e.,  $\log K_j = x_j^T \beta$ ) and  $\Delta(\log K)$  is half  
 129 the width of the PI.  $\Delta(\log K)$  is calculated as,

$$130 \quad \Delta(\log K) = t_{\alpha/2, n-k-1} \text{SD}_{\text{training}} \sqrt{1 + x_j^T (X^T X)^{-1} x_j} \quad (6)$$

$$131 \quad = t_{\alpha/2, n-k-1} \text{SD}_{\text{training}} \sqrt{1 + h} \quad (7)$$

132 where  $t_{\alpha/2, n-k-1}$  is the two-tailed  $t$ -value for a given confidence level ( $\alpha$ , e.g., 95%), number of  
 133 training data ( $n$ ), and number of independent variables ( $k$ ; 5 for PP-LFERs).  $\text{SD}_{\text{training}}$  is the  
 134 standard deviation of the PP-LFER model fitted to the training data.  $\Delta(\log K)$  may be  
 135 normalized to  $\text{SD}_{\text{training}}$ , as

$$136 \quad \Delta(\log K) / \text{SD}_{\text{training}} = t_{\alpha/2, n-k-1} \sqrt{1 + h} \quad (8)$$

137 In this study, the following two tests were performed to discuss the use of  $h$  and the  
 138 PIs to delineate the AD of PP-LFERs.

## 139 **2.2 Test 1: Comparison of prediction errors with $h$ and the PIs**

140 In the first test, the variation of actual prediction errors by PP-LFERs with  $h$  and the PIs was  
 141 examined. Six experimental data sets of partition coefficients from existing literature were  
 142 used: octanol/water ( $K_{\text{ow}}$ ,  $n = 314$ );<sup>10</sup> air/water ( $K_{\text{aw}}$ ,  $n = 390$ );<sup>11</sup> oil/water ( $K_{\text{oilw}}$ ,  $n = 247$ );<sup>12</sup> soil  
 143 organic carbon/water ( $K_{\text{oc}}$ ,  $n = 79$ );<sup>13</sup> phospholipid liposome/water ( $K_{\text{lipw}}$ ,  $n = 131$ );<sup>14</sup> and  
 144 bovine serum albumin/water ( $K_{\text{BSAw}}$ ,  $n = 82$ ).<sup>15</sup> These data sets comprise a relatively large

145 number of compounds and exhibit environmental and toxicological relevance.  $K_{ow}$ ,  $K_{aw}$ , and  
146  $K_{oilw}$  were partition coefficients between two homogeneous solvents, whereas  $K_{oc}$ ,  $K_{lipw}$ , and  
147  $K_{BSAw}$  involved a heterogeneous or anisotropic phase. The  $K$  values and solute descriptors  
148 were obtained from the aforementioned references, are listed in Tables S1–S6, and are summarized  
149 in Table S7 (SI-2 of the SI)

150 To evaluate prediction accuracy, the  $K$  data of each set were divided into training and  
151 test sets. Training compounds were randomly selected from the entire data set. The number  
152 of the training compounds ( $n_{training}$ ) was 20, 30, 40, 50, 75 or 100. Rather small values of  $n_{training}$   
153 were also included in this test to simulate cases of insufficient calibration. The compounds  
154 that were not selected as training compounds were used as test compounds. The PP-LFER in  
155 the form of eq 1 was calibrated with the training data and was used to predict  $\log K$  for the  
156 test compounds. Prediction errors (predicted  $\log K$  – experimental  $\log K$ ) were calculated and  
157 compared with  $h$  and  $\Delta(\log K)$ . For each combination of the  $K$  set and  $n_{training}$ , the cycle of  
158 “random generation of a training set,” “calibration of the PP-LFER,” and “prediction for the  
159 test set” was repeated 200 times. This number was arbitrary but appeared sufficient for stable  
160 results.

161 Additionally, using the 200 calibrated PP-LFERs for each case, the experimental  $\log K$   
162 values of per- and polyfluoroalkyl substances (PFASs) and organosilicon compounds (OSCs)  
163 were predicted. PFASs and OSCs possess extremely weak van der Waals interaction  
164 properties; thus, the  $E$  and  $L$  values are comparatively low for their molecular sizes.<sup>16</sup>  
165 Therefore, PP-LFERs often have to be extrapolated to predict  $K$  values. These classes of  
166 compounds are not present in the data set of any considered PP-LFER and are used to  
167 evaluate the influences of extrapolation on the prediction accuracy.

168 All calculations mentioned above were performed with  $R$  software.

### 169 **2.3 Test 2: Evaluating reported PP-LFERs with AD probes**

170 In the second test,  $h$  and PI calculation was applied to evaluate the AD of reported PP-LFER  
171 equations. Here,  $n$ ,  $SD_{training}$ , and the solute descriptors of the calibration compounds were  
172 extracted from existing literature and used to calculate  $h$  and PIs for 25 selected compounds  
173 (Table S8, SI-3). These compounds, referred to as AD probes herein, were selected because  
174 of their wide variations in descriptor values, structural diversity, and environmental relevance.  
175 They represented aliphatic and aromatic, polar and nonpolar, and small and large compounds

176 and included multifunctional polar compounds such as various pesticides and  
177 pharmaceuticals, a neutral PFAS, and an OSC. Solute descriptors for the AD probes were  
178 obtained from the UFZ-LSER database and listed in Table S8 (SI-3).<sup>17</sup> Test 2 did not require the  
179 experimental  $K$  values of the AD probes, and only solute descriptors were used for the  
180 calculation. As the SI, an Excel file with a macro is provided that calculates  $h$ ,  $h/h_{\text{mean}}$ , and  
181  $\Delta(\log K)$  for the AD probes and any desired chemical based on the user-entered training data.  
182 Note that there exist compounds with extreme descriptor values that are not covered by the  
183 25 AD probes proposed here. For example, an antibiotic erythromycin ( $E = 2.90$ ,  $S = 3.73$ ,  $A =$   
184  $1.25$ ,  $B = 4.96$ ,  $V = 5.773$ )<sup>18</sup> exhibits exceptionally high  $S$ ,  $B$  and  $V$  values. However, such  
185 compounds are rarely used for calibration and are always out of the calibration domain;  
186 therefore, they are not necessary specifically in this evaluation.

187

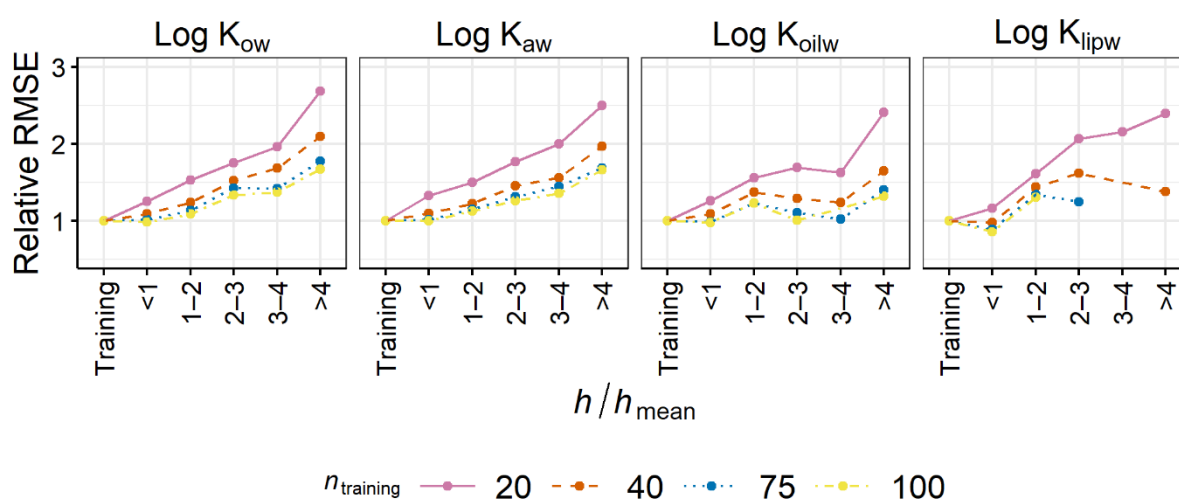
### 188 **3. Results and discussion**

#### 189 **3.1 Prediction errors compared to $h$ and the PIs (Test 1)**

190 Figure S1 (SI-4) shows the root mean squared errors (RMSEs) for training and testing sets  
191 randomly generated 200 times. The test compounds were grouped into several bins according  
192 to the  $h$  normalized to  $h_{\text{mean}}$  ( $h/h_{\text{mean}}$ ) before the RMSEs were calculated. The observed RMSE  
193 for the test compounds increased with  $h$  for a given  $K$  data set and  $n_{\text{training}}$ . The increasing  
194 trend of RMSE with  $h$  was particularly clear for simulations with small  $n_{\text{training}}$  values (i.e., 20,  
195 30). The trend was sometimes unclear for simulations with high  $n_{\text{training}}$  values, likely because  
196 large  $n_{\text{training}}$  resulted in a relatively small  $n_{\text{test}}$ , which may not be able to provide  
197 representative RMSEs, particularly for high  $h/h_{\text{mean}}$  bins.

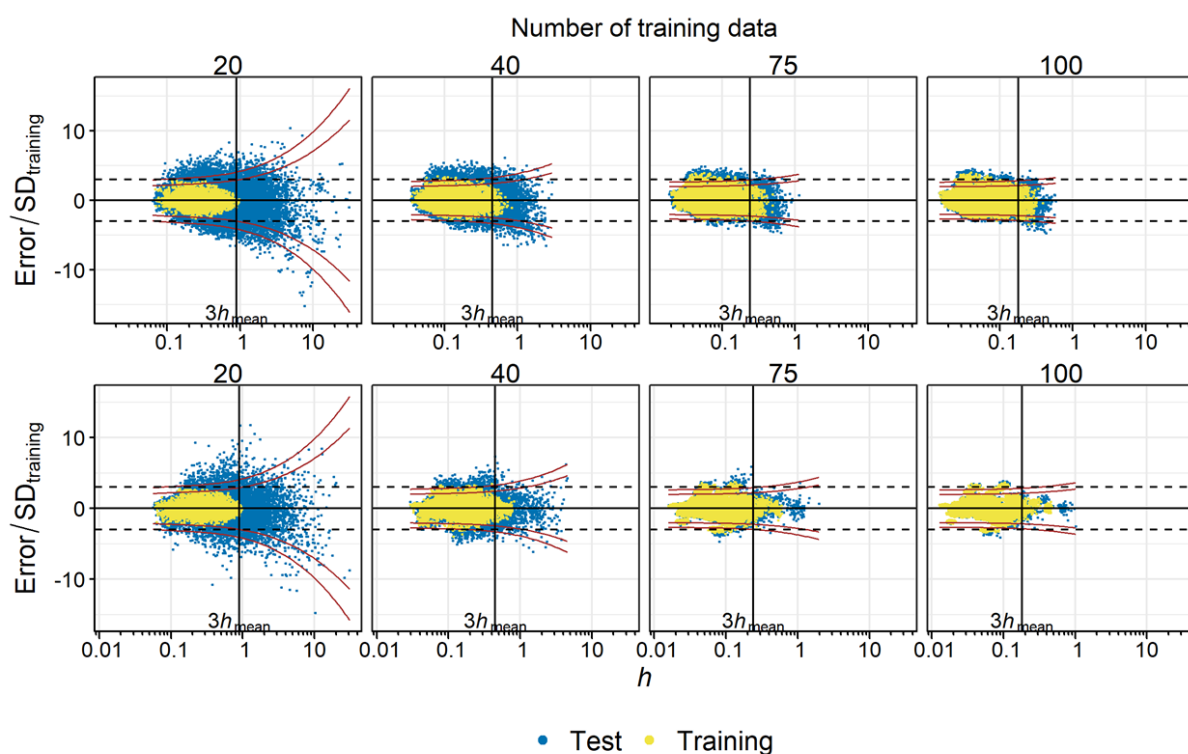
198 To demonstrate the increase in RMSE with  $h/h_{\text{mean}}$  more clearly, the RMSE values for  
199 the test data relative to the RMSE for the training data were calculated (Figure 1, Figure S2 in  
200 SI-4). The relative RMSE generally increased with  $h/h_{\text{mean}}$  but to a lesser extent when  $n_{\text{training}}$   
201 was large. For example, the relative RMSEs of  $\log K_{\text{ow}}$  data in the “ $2 < h/h_{\text{mean}} < 3$ ” bin were  
202 1.75, 1.52, 1.42, and 1.34 for  $n_{\text{training}} = 20, 40, 75,$  and  $100$ , respectively. This result suggests  
203 that if the PP-LFER is trained with a sufficient size of data, the RMSEs for interpolations (i.e.,  
204  $h/h_{\text{mean}} < 3$ ) will resemble the RMSE for the training set. Noteworthy, even for the “ $3 <$   
205  $h/h_{\text{mean}} < 4$ ” bin (i.e., extrapolation), the relative RMSE for any  $K$  considered was  $< 1.5$  when  
206  $n_{\text{training}} \geq 50$ , and  $< 2.2$  when  $n_{\text{training}} \geq 20$ . These RMSEs can be sufficiently accurate for various

207 purposes. Although  $h = 3h_{\text{mean}}$  is the common definition of extrapolation, the actual threshold  
 208 of  $h$  may be adapted to the required accuracy of predictions, depending on the quality of the  
 209 PP-LFER fit and  $n_{\text{training}}$ . For example, if the required accuracy is 0.3 log units, which is typically  
 210 the level of accuracy of contaminant fate models,<sup>19</sup> then extrapolations by the PP-LFERs for  
 211  $\log K_{\text{ow}}$  and  $\log K_{\text{aw}}$  up to an  $h/h_{\text{mean}}$  of 4 can be allowed, according to the results of Test 1  
 212 (Figure S1). In contrast, a stricter threshold, e.g.,  $h/h_{\text{mean}} < 2$  or even  $< 1$ , should be set to  $\log$   
 213  $K_{\text{oc}}$ ,  $\log K_{\text{lipw}}$ , and  $\log K_{\text{BSAw}}$  to comply with the criterion of 0.3 log unit RMSE. Alternative AD  
 214 thresholds are further discussed in Section 3.3.



215  
 216 **Figure 1. RMSEs of the test data, sorted according to  $h/h_{\text{mean}}$ , relative to the RMSE of the**  
 217 **training data. The plots for  $n_{\text{training}} = 30$  and  $50$  and  $\log K_{\text{oc}}$  and  $\log K_{\text{BSAw}}$  are available in the**  
 218 **Figure S2 (SI-4).**

219  
 220  
 221 Along with average errors, such as RMSEs, the risk of an extremely inaccurate  
 222 prediction is of interest. Individual data of Test 1 for  $\log K_{\text{ow}}$  and  $\log K_{\text{lipw}}$  were plotted against  
 223  $h$  (Figure 2). All other data are shown in Figure S3 (SI-5). When  $n_{\text{training}}$  was small (e.g., 20, 30),  
 224 both  $h$  (x-axis) and prediction errors (y-axis, normalized to  $SD_{\text{training}}$ ) for the test data were  
 225 widely distributed. Extremely large errors ( $|\text{error}/SD_{\text{training}}| > 5$ ) occasionally occurred,  
 226 particularly if  $h$  was large ( $> 10h_{\text{mean}}$ ). In contrast, when  $n_{\text{training}}$  was large (e.g., 75, 100), the  
 227 training and test data were similarly distributed in terms of  $h$  and the prediction errors.  
 228



229

230 **Figure 2. Prediction errors normalized to  $SD_{\text{training}}$  plotted against  $h$ . Results from 200**  
 231 **simulations are shown. The vertical line indicates  $3h_{\text{mean}}$ . The dashed horizontal lines**  
 232 **indicate errors that are 3 times the  $SD_{\text{training}}$ . The curves indicate the 95% (inside) and 99%**  
 233 **(outside) prediction intervals. Top,  $\log K_{\text{ow}}$ ; bottom,  $\log K_{\text{lipw}}$ . All other data are shown in**  
 234 **Figure S3 (SI-5).**

235

236

237 The percentage of large prediction errors, defined by  $|\text{error}/SD_{\text{training}}| > 3$ , was  
 238 generally higher for extrapolation ( $h/h_{\text{mean}} > 3$ ) than interpolation ( $h/h_{\text{mean}} < 3$ ) (Figure S4, SI-  
 239 6). However, the percentage strongly decreased with  $n_{\text{training}}$ . As an example: for  $\log K_{\text{ow}}$ , when  
 240  $n_{\text{training}} = 20$ , 3.3% of the interpolations and 17% of the extrapolations suffered from large  
 241 prediction errors. In contrast, when  $n_{\text{training}} = 100$ , 0.94% of the interpolations and 4.7% of the  
 242 extrapolations resulted in large prediction errors, which conversely indicated that 94% of the  
 243 extrapolations ended up with errors within 3  $SD_{\text{training}}$ .

244 Figures 2 additionally shows the 95% and 99% PIs as a function of  $h$ . The PIs were  
 245 narrow up to  $h \sim 1$  and diverged with  $h$ , as expected from eq 8. The extent of divergence was  
 246 large when  $n_{\text{training}}$  was small, which can be explained by a large  $t_{\alpha/2, n-k-1}$  in eq 8. The data points  
 247 from Test 1 were within the PIs with a few outliers. The percentage of the test data within a

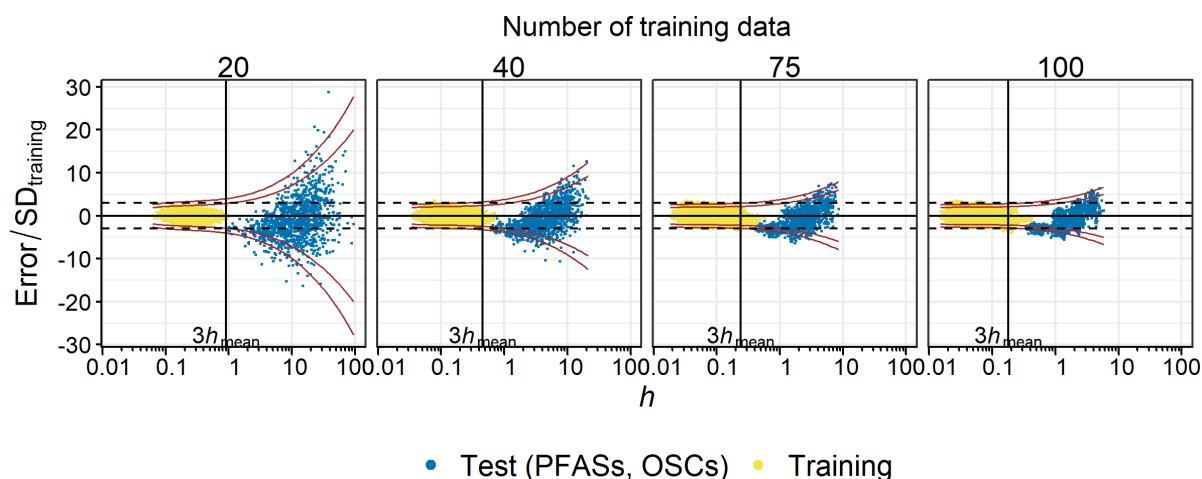
248 given PI agrees with the theoretical expectations; e.g., ca 95% of the test data are within the  
249 95% PI, independent of  $n_{\text{training}}$  (Figure S5, SI-7).

250 Overall, Test 1 demonstrated that the mean prediction error increased with  $h$  and  
251 could be used to identify “risky predictions” that frequently cause high inaccuracy. However,  
252 a threshold of  $3h_{\text{mean}}$  did not appear to be versatile in defining the AD, as the  $n_{\text{training}}$  appeared  
253 to influence the range of prediction errors. The plots in Figures 1, 2, and S1–S5 suggested that,  
254 when  $n_{\text{training}}$  was large,  $h = 3h_{\text{mean}}$  might be overly strict as a threshold, because prediction  
255 errors were often similar in magnitude even when  $h > 3h_{\text{mean}}$ . Note that Test 1 was also  
256 performed with eq 3, the PP-LFER equation that uses  $L$  instead of  $E$ . However, the results were  
257 similar to those of eq 1 and are thus not discussed herein.

258

### 259 3.2 PFASs and OSCs

260 Using 200 trained PP-LFERs, log  $K_{\text{ow}}$  of 3 PFASs (4:2 fluorotelomer alcohol (FTOH), 6:2 FTOH,  
261 and 8:2 FTOH) and 3 OSCs (octamethylcyclotetrasiloxane (D4), decamethylcyclopentasiloxane  
262 (D5), and dodecamethylcyclohexasiloxane (D6)) were predicted and compared to the  
263 experimental data (Figure 3; additional data in Figure S6, SI-8.<sup>16</sup> For this comparison, eq 3  
264 instead of eq 1 was used because the latter is known to be unsuitable for PFASs and OSCs (ref  
265 16; also compare Figures S6 and S7 in SI-8 and SI-9, respectively). The  $h/h_{\text{mean}}$  ratios for these  
266 six chemicals were always above 3 with any  $n_{\text{training}}$  used and were up to 300, indicating strong  
267 extrapolations. The predictions were highly inaccurate when the  $n_{\text{training}}$  was small. However,  
268 the predictions appeared to improve with an increase in  $n_{\text{training}}$ . When  $n_{\text{training}} = 100$ , even  
269 largely extrapolated FTOHs ( $h \sim 2$ ,  $h/h_{\text{mean}} \sim 33$ ) were frequently predicted within  $3 \text{SD}_{\text{training}}$ .  
270 The dependence of the prediction error on  $h$  was well captured by the PIs; the majority of the  
271 data were within the 99% PIs, and this was the case for extreme extrapolations as well (Figures  
272 3, S6). The results for PFASs and OSCs can be considered another indication that well-  
273 calibrated PP-LFERs are robust against extrapolation and that  $h = 3h_{\text{mean}}$  as the cutoff criterion  
274 is excessively strict if the  $n_{\text{training}}$  is large. Notably, although well-calibrated PP-LFERs appear  
275 to bear extrapolation, the inclusion of PFASs and OSCs in the calibration set is the first choice  
276 to develop PP-LFERs that work for these classes of chemicals, as that substantially decreases  
277  $h$  for PFASs and OSCs.<sup>16</sup>



278  
 279 **Figure 3. Prediction errors for  $\log K_{\text{ow}}$  of PFAS and OSCs normalized to  $SD_{\text{training}}$  plotted**  
 280 **against  $h$ . The results from 200 simulations are shown. The lines indicate the same as in**  
 281 **Figure 2. Equation 3 was used for this plot (see text for more details). Additional data are in**  
 282 **Figure S6 (SI-8).**

283

### 284 3.3 How can we define the AD of PP-LFERs?

285 In previous discussions regarding the AD of quantitative structure activity relationships  
 286 (QSARs), the use of  $h$  with a cutoff value of  $3h_{\text{mean}}$  has been frequently presented. As shown  
 287 in Test 1 of this study, however, this cutoff may excessively limit the potential of well-  
 288 calibrated PP-LFERs to predict a broad range of compounds above the  $3h_{\text{mean}}$  threshold. The  
 289 use of the PI, in contrast, has rarely been investigated in the context of QSAR development  
 290 but may be more practical for multiple linear regression models, such as PP-LFERs, because  
 291 the PI encompasses the distance ( $h$ ), quality of model fit ( $SD_{\text{training}}$ ), and size of training data  
 292 (influencing  $h$  and  $t_{\alpha/2, n-k-1}$ ) and provides a concrete estimate of the error range (eq 7). To use  
 293 the PI to define the AD, an upper threshold for  $\Delta(\log K)$  must be set. Here, two ways that may  
 294 be acceptable are discussed.

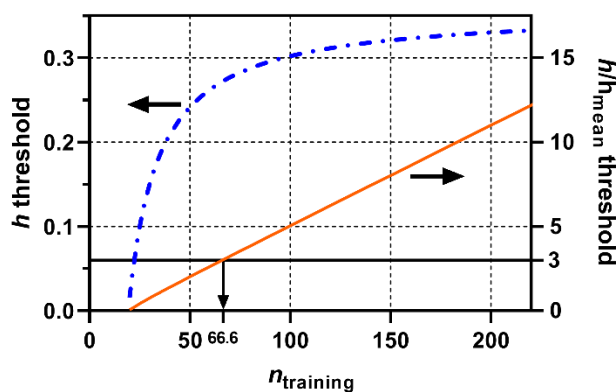
295 (A) Set the  $\Delta(\log K)$  threshold at a multiple of  $SD_{\text{training}}$ . The AD may be defined by a  
 296  $\Delta(\log K)$  threshold that is a multiple of  $SD_{\text{training}}$ . An example of such a criterion is  $\Delta(\log K)_{99\%PI}$   
 297  $< 3SD_{\text{training}}$ . According to eq 8, this condition corresponds to,

$$298 \quad t_{99/2, n-k-1} \sqrt{1+h} < 3 \quad (9)$$

299 Inequality 9 describes the two intersections in Figures 2 and 3 where the curves for the 99%  
 300 PI meet the horizontal lines for  $\pm 3SD_{\text{training}}$ . By solving this inequality for  $h$ , we obtain,

301 
$$h < \left( \frac{3}{t_{99/2, n-k-1}} \right)^2 - 1 \quad (10)$$

302 Inequality 10 describes a new  $h$  threshold that is derived from “ $\Delta(\log K)_{99\%PI} < 3SD_{\text{training}}$ ” and  
 303 is a function of  $t_{\alpha/2, n-k-1}$ . As  $t_{\alpha/2, n-k-1}$  is dependent on  $n_{\text{training}}$ , this  $h$  threshold is also dependent  
 304 on  $n_{\text{training}}$  (Figure 4). For example, if  $n_{\text{training}} = 50$ , the new threshold is  $h < 0.24$ , which is  $h/h_{\text{mean}} < 2.0$ . If  $n_{\text{training}} = 100$ , the threshold is  $h < 0.30$ , which is  $h/h_{\text{mean}} < 5.0$ . The common threshold  
 305  $h/h_{\text{mean}} < 3$  can be derived when  $n_{\text{training}} = 66.6$ . Thus, the new threshold is stricter if  $n_{\text{training}} < 66.6$   
 306 and less strict if  $n_{\text{training}} > 66.6$ , compared with the  $3h_{\text{mean}}$  rule.



308  
 309 **Figure 4. New thresholds of  $h$  and  $h/h_{\text{mean}}$  derived from  $\Delta(\log K)_{99\%PI} < 3SD_{\text{training}}$  as a criterion**  
 310 **(eq 10).**

311  
 312 (B) Set the  $\Delta(\log K)$  threshold at a certain value. In the second approach, the AD is  
 313 defined in such a way that the PI becomes narrower than a certain range. For example, we  
 314 may consider  $\Delta(\log K)_{99\%PI} < 0.5$  (i.e., a factor of 3 for  $K$ ) as an acceptable error margin, then  
 315 eq 7 becomes,

316 
$$t_{99/2, n-k-1} SD_{\text{training}} \sqrt{1+h} < 0.5 \quad (11)$$

317 which can be rewritten as,

318 
$$h < \left( \frac{0.5}{t_{99/2, n-k-1} SD_{\text{training}}} \right)^2 - 1 \quad (12)$$

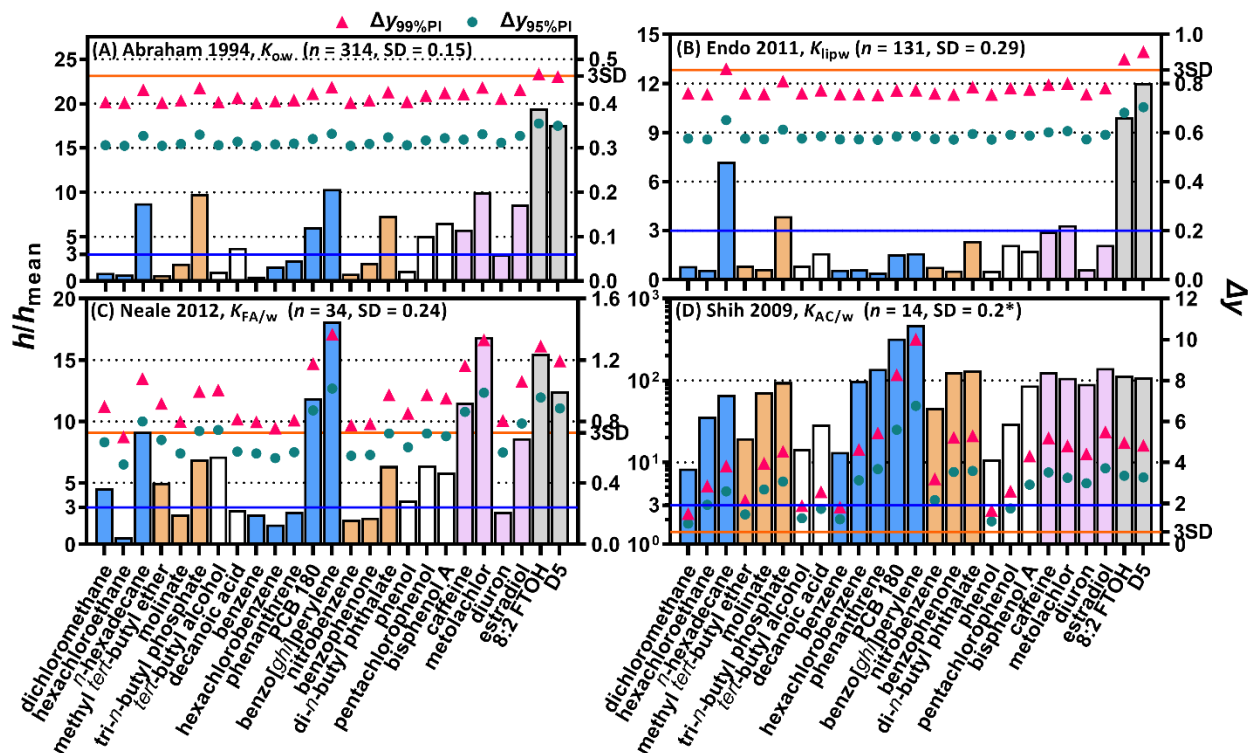
319 Using the  $SD_{\text{training}}$  value for the PP-LFER of  $\log K_{\text{ow}}$  (Table S7, SI-1) as an example, we can  
 320 derive a threshold of  $h$  specific to  $\log K_{\text{ow}}$ . By inserting  $SD_{\text{training}} = 0.154$  and  $t_{99/2, n-k-1} = 2.59$   
 321 (with  $n = 314$ ) in inequality 12, we obtained  $h < 0.57$  (i.e.,  $h/h_{\text{mean}} < 30$ ). Note that if  $SD_{\text{training}}$   
 322 is high (e.g., 0.285 for  $\log K_{\text{lipw}}$ ), “ $\Delta(\log K)_{99\%PI} < 0.5$ ” is not achievable no matter how large  
 323  $n_{\text{training}}$  is, because  $t_{99/2, n-k-1}$  is  $> 2.58$  regardless of  $n_{\text{training}}$  and the righthand side of inequality

324 12 is always negative. The difficulty associated with this approach to define the AD may be to  
 325 set the acceptable  $\Delta(\log K)_{99\%PI}$  level such that it is both useful and achievable.

326

### 327 3.4 Evaluating AD of published PP-LFERs with AD probes (Test 2)

328 Using the 25 AD probes, 10 published PP-LFER equations<sup>10-15,20-23</sup> including those used in Test  
 329 1 were evaluated (Figure 5, Figure S8 in SI-10).



330  
 331 **Figure 5. Leverage (bars) and prediction intervals (triangles and circles) of 25 applicability**  
 332 **domain (AD) probes calculated with the training data sets of four PP-LFERs. Solid horizontal**  
 333 **lines indicate  $h/h_{\text{mean}} = 3$  and  $\Delta(\log K) = 3SD$ . \*The cited reference does not give SD but a**  
 334 **“mean error” of 0.2, which was used here. Plots for all 10 PP-LFERs are shown in Figure S8,**  
 335 **SI-10.**

336

337 The  $h$  calculation showed that none of the 10 training sets considered encompassed  
 338 all the 25 AD probes within the  $3h_{\text{mean}}$  domain. This indicates that certain environmentally  
 339 relevant compounds must be extrapolated with these PP-LFERs. Particularly, 8:2 FTOH and D5  
 340 always appeared as highly extrapolated chemicals ( $h/h_{\text{mean}} = 8-50$ ), reflecting the fact that  
 341 PFASs and OSCs were not included in any of the training sets and indicating that these

342 compounds were not well represented by other training compounds. For each type of  
343 chemical, the small compounds (e.g., dichloromethane, methyl *tert*-butyl ether, benzene)  
344 exhibited lower  $h/h_{\text{mean}}$  ratios than the large compounds (e.g., hexadecane, tri-*n*-butyl  
345 phosphate, benzo[*ghi*]perylene). Generally, relatively small compounds are easy to measure,  
346 and their data are present in the training set, whereas obtaining data for large compounds  
347 tends to be more challenging. Consequently, PP-LFERs must be frequently extrapolated for  
348 large compounds.

349 The data sets for  $\log K_{\text{ow}}^{10}$  and  $\log K_{\text{aw}}^{11}$  exhibited similar patterns for  $h/h_{\text{mean}}$  and  $\Delta(\log K)$ .  
350 Thus, the  $h/h_{\text{mean}}$  ratios of the small compounds were  $< 3$  (interpolation) and those of the  
351 large compounds were in the range of 3–15 (extrapolation) (Figure 5A). However, the  $\Delta(\log K)$   
352 values were not largely different across the 25 AD probes. Although 12 out of 25 AD probes  
353 exhibited  $h/h_{\text{mean}} > 3$ ,  $\Delta(\log K)_{95\%PI}$  and  $\Delta(\log K)_{99\%PI}$  were  $\sim 0.3$  and  $\sim 0.4$ , respectively, for all  
354 the AD probes. Even for strongly extrapolated 8:2 FTOH,  $\Delta(\log K)_{95\%PI}$  and  $\Delta(\log K)_{99\%PI}$  of  $\log$   
355  $K_{\text{ow}}$  predictions were 0.36 and 0.47, respectively. These relatively low  $\Delta(\log K)$  values for the  
356 extrapolated compounds originated from the substantial size of training data for  $K_{\text{ow}}$  and  $K_{\text{aw}}$ .  
357 The  $\log K_{\text{oilw}}^{12}$  data set resulted in similar patterns for  $h/h_{\text{mean}}$  and  $\Delta(\log K)$ , but the values of  
358  $\Delta(\log K)$  were higher than those of  $\log K_{\text{ow}}$  and  $\log K_{\text{aw}}$  because of the higher  $SD_{\text{training}}$  of  $\log$   
359  $K_{\text{oilw}}$  (Figure S8).

360 The data set for  $\log K_{\text{lipw}}^{14}$  had the benefit of excellent coverage of the AD probes; only  
361 5 out of 25 AD probes exhibited  $h/h_{\text{mean}} > 3$  (Figure 5B). A wealth of data for hydrophobic  
362 compounds (e.g., PAHs), substituted phenols, hormones, and pharmaceuticals in addition to  
363 simple aliphatic and aromatic and polar and nonpolar compounds with varying sizes resulted  
364 in the low  $h/h_{\text{mean}}$  for the AD probes. Because of the low  $h/h_{\text{mean}}$  and high  $n$ , the  $\Delta(\log K)$  values  
365 were similar for all AD probes. Nevertheless, the values of  $\Delta(\log K)_{95\%PI}$  and  $\Delta(\log K)_{99\%PI}$  ( $\sim 0.6$   
366 and  $\sim 0.8$ , respectively) for  $\log K_{\text{lipw}}$  were higher than those for  $\log K_{\text{ow}}$  by a factor of  $\sim 2$ ,  
367 because the  $SD_{\text{training}}$  of  $\log K_{\text{lipw}}$  was higher by the same factor.

368 Figures 5C and 5D show illustrative examples of PP-LFERs with limited training data.  
369 The data set of fulvic acid/water partition coefficients ( $K_{\text{FA/w}}^{20}$ ) comprised 34 training data,  
370 and 16 out of 25 AD probes were extrapolated ( $h/h_{\text{mean}} > 3$ ). The major difference from  $\log$   
371  $K_{\text{ow}}$  and  $\log K_{\text{lipw}}$  was the wide range of  $\Delta(\log K)$ ; the  $\Delta(\log K)_{95\%PI}$  and  $\Delta(\log K)_{99\%PI}$  values for  
372  $\log K_{\text{FA/w}}$  were in the range of 0.5–1.0 and 0.7–1.4, respectively. The data set of activated  
373 carbon/water partition coefficients ( $K_{\text{AC/w}}^{23}$ ) was a clearer example of insufficient calibration.

374 It only contained 14 training data, and all AD probes were considered extrapolated ( $h/h_{\text{mean}}$ ,  
375 8–480). Although the model fitting seemed to be good (the stated mean error, 0.2),<sup>23</sup> the PIs  
376 were extremely broad, with  $\Delta(\log K)_{95\%PI}$  and  $\Delta(\log K)_{99\%PI}$  being 1.0–6.8 and 1.5–10,  
377 respectively. These results indicate that PP-LFERs from such small training sets will have a  
378 limited predictive ability for external compounds. Conversely, the calculation of  $h$  and the PIs  
379 will be most useful for such poorly calibrated PP-LFERs, as they can identify compounds for  
380 which the precision of prediction is still acceptable.

381 In SI-10 of the SI, a comparative discussion is provided for three data sets of log  
382  $K_{oc}$ <sup>13,21,22</sup> in terms of their ADs. These data sets possessed different characteristics, which were  
383 demonstrated by the AD probes.

384 Overall, it can be concluded that the 25 AD probes are useful in illustrating the  
385 strength and weakness of calibrated PP-LFERs. The missing classes of compounds in the  
386 training data, e.g., large hydrophobic compounds and multifunctional polar compounds, can  
387 be identified using the  $h/h_{\text{mean}}$  values, and the associated elevation of error margins can be  
388 evaluated by calculating the PIs.

389

### 390 **3.5 Practical implications**

391 This study demonstrated that extrapolation was error-prone when the number of training  
392 data was limited and the  $h/h_{\text{mean}}$  value was extremely high. In contrast, well-calibrated PP-  
393 LFERs with many training data (e.g., 100) were highly robust against extrapolation. For  
394 partition coefficients between solvent phases or solvent and air such as  $K_{ow}$  and  $K_{aw}$ , the data  
395 are typically accurate and abundant. Thus, extrapolations can frequently result in low  
396 prediction errors. Extrapolation matters for heterogeneous environmental, biological, and  
397 technical phases, because the data are often limited, and  $SD_{\text{training}}$  tends to be large.

398 The commonly used threshold of  $h < 3 h_{\text{mean}}$  appeared not to be useful in defining the  
399 AD of PP-LFER models. Alternatively, two possible ways were proposed in this article to define  
400 the AD based on the calculation of the PI. For practical purposes, presenting the PIs for each  
401 time of prediction may be highly recommended. For example, using the PP-LFER, log  $K_{ow}$  for  
402 hexachlorobenzene is predicted as 5.49 with a 95% PI of [5.16, 5.81]. With these PI values,  
403 the model user can appreciate the reliability of the prediction and decide whether the value  
404 is taken or not, following the accuracy required for the given model use. It could be claimed

405 that calculating the PI each time is more important and useful than seeking a strict definition  
406 of the AD, because the former presents a quantitative estimate of the error range, while the  
407 latter is a qualitative, binomial indicator with an arbitrary cutoff in the end.

408 To develop a robust PP-LFER, the training set should contain (A) a large number (>60,  
409 preferably >100) of (B) accurate experimental  $K$  data for (C) diverse compounds with (D)  
410 accurate descriptors available. (A) decreases  $t_{\alpha/2, n-k-1}$  and  $h$ , (B) and (D) decrease  $SD_{\text{training}}$ , and  
411 (C) decreases  $h$  in eq 7, all contributing to tight PIs. The predictive performance of an empirical  
412 model is always restricted by the quality and quantity of the underlying experimental data.  
413 The improvement in data accuracy and availability will contribute to the further development  
414 of PP-LFER approaches.

415 Extended use of the PI may be considered for evaluating the AD of QSARs that are  
416 derived by the multiple linear regression analysis. The calculation of the PI is no more complex  
417 than  $h$  is, but the former provides far more insights into the reliability of predictions, as  
418 discussed above. Noteworthy, the success of applying the PI for PP-LFERs may be partially  
419 related to the excellent linearity of the PP-LFER descriptors to  $\log K$ . The suitability of the PI  
420 for various existing QSAR descriptors and properties warrants future investigation.

421

## 422 **Associated content**

423 Supporting information

424 The Supporting Information is available free of charge at ...

425 Additional explanations for  $h$  and PIs, tables listing the used  $K$  data and AD probes, additional  
426 figures for Tests 1 and 2 (PDF)

427 MS Excel file with a macro to calculate  $h$  and the PIs (XLSM)

428

## 429 **Conflicts of interest**

430 The author has no conflicts of interest associated with this article.

431

## 432 **Acknowledgments**

433 This work was supported by JSPS KAKENHI Grant Numbers JP18K05204 and JP16K16216 and  
434 by the MEXT/JST Tenure Track Promotion Program. Kai-Uwe Goss and Jort Hammer are  
435 thanked for their valuable comments on an earlier version of this manuscript.

436

## 437 **References**

- 438 1. Abraham, M. H.; Ibrahim, A.; Zissimos, A. M., Determination of sets of solute  
439 descriptors from chromatographic measurements. *J. Chromatogr. A* **2004**, *1037*, (1-2), 29-47.
- 440 2. Goss, K.-U.; Schwarzenbach, R. P., Linear free energy relationships used to evaluate  
441 equilibrium partitioning of organic compounds. *Environ. Sci. Technol.* **2001**, *35*, (1), 1-9.
- 442 3. Endo, S.; Goss, K.-U., Applications of Polyparameter Linear Free Energy Relationships  
443 in Environmental Chemistry. *Environ. Sci. Technol.* **2014**, *48*, (21), 12477-12491.
- 444 4. Poole, C. F.; Ariyasena, T. C.; Lenca, N., Estimation of the environmental properties of  
445 compounds from chromatographic measurements and the solvation parameter model. *J.*  
446 *Chromatogr. A* **2013**, *1317*, 85-104.
- 447 5. Goss, K.-U., Predicting the equilibrium partitioning of organic compounds using just  
448 one linear solvation energy relationship (LSER). *Fluid Phase Equilib.* **2005**, *233*, (1), 19-22.
- 449 6. Netzeva, T. I.; Worth, A.; Aldenberg, T.; Benigni, R.; Cronin, M. T.; Gramatica, P.;  
450 Jaworska, J. S.; Kahn, S.; Klopman, G.; Marchant, C. A.; Myatt, G.; Nikolova-Jeliazkova, N.;  
451 Patlewicz, G. Y.; Perkins, R.; Roberts, D.; Schultz, T.; Stanton, D. W.; van de Sandt, J. J.; Tong,  
452 W.; Veith, G.; Yang, C., Current status of methods for defining the applicability domain of  
453 (quantitative) structure-activity relationships. The report and recommendations of ECVAM  
454 Workshop 52. *ATLA Altern. Lab. Anim.* **2005**, *33*, (2), 155-73.
- 455 7. Jaworska, J.; Nikolova-Jeliazkova, N.; Aldenberg, T., QSAR Applicability Domain  
456 Estimation by Projection of the Training Set in Descriptor Space: A Review. *ATLA Altern. Lab.*  
457 *Anim.* **2005**, *33*, (5), 445-459.
- 458 8. Gramatica, P., Principles of QSAR models validation: internal and external. *QSAR Comb*  
459 *Sci.* **2007**, *26*, (5), 694-701.
- 460 9. Gramatica, P.; Giani, E.; Papa, E., Statistical external validation and consensus  
461 modeling: A QSPR case study for  $K_{oc}$  prediction. *J. Mol. Graph. Model.* **2007**, *25*, (6), 755-766.
- 462 10. Abraham, M. H.; Chadha, H. S.; Whiting, G. S.; Mitchell, R. C., Hydrogen bonding. 32.  
463 An analysis of water-octanol and water-alkane partitioning and the  $\Delta \log P$  parameter of seiler.  
464 *J. Pharm. Sci.* **1994**, *83*, (8), 1085-100.

- 465 11. Abraham, M. H.; Andonian-Haftvan, J.; Whiting, G. S.; Leo, A.; Taft, R. S., Hydrogen  
466 bonding. Part 34. The factors that influence the solubility of gases and vapors in water at 298  
467 K, and a new method for its determination. *J. Chem. Soc. Perkin Trans. 2* **1994**, (8), 1777-91.
- 468 12. Geisler, A.; Endo, S.; Goss, K.-U., Partitioning of Organic Chemicals to Storage Lipids:  
469 Elucidating the Dependence on Fatty Acid Composition and Temperature. *Environ. Sci.*  
470 *Technol.* **2012**, *46*, (17), 9519-9524.
- 471 13. Bronner, G.; Goss, K.-U., Predicting sorption of pesticides and other multifunctional  
472 organic chemicals to soil organic carbon. *Environ. Sci. Technol.* **2011**, *45*, (4), 1313-1319.
- 473 14. Endo, S.; Escher, B. I.; Goss, K.-U., Capacities of Membrane Lipids to Accumulate  
474 Neutral Organic Chemicals. *Environ. Sci. Technol.* **2011**, *45*, (14), 5912-5921.
- 475 15. Endo, S.; Goss, K.-U., Serum Albumin Binding of Structurally Diverse Neutral Organic  
476 Compounds: Data and Models. *Chem. Res. Toxicol.* **2011**, *24*, (12), 2293-2301.
- 477 16. Endo, S.; Goss, K.-U., Predicting Partition Coefficients of Polyfluorinated and  
478 Organosilicon Compounds using Polyparameter Linear Free Energy Relationships (PP-LFERs).  
479 *Environ. Sci. Technol.* **2014**, *48*, (5), 2776-2784.
- 480 17. Ulrich, N.; Endo, S.; Brown, T. N.; Watanabe, N.; Bronner, G.; Abraham, M. H.; Goss, K.  
481 U., UFZ-LSER database v 3.2 [Internet]. **2017**.
- 482 18. Abraham, M. H.; Ibrahim, A.; Acree, W. E., Jr., Air to lung partition coefficients for  
483 volatile organic compounds and blood to lung partition coefficients for volatile organic  
484 compounds and drugs. *Eur. J. Med. Chem.* **2008**, *43*, (3), 478-485.
- 485 19. Mackay, D.; Arnot, J. A., The Application of Fugacity and Activity to Simulating the  
486 Environmental Fate of Organic Contaminants. *J. Chem. Eng. Data* **2011**, *56*, (4), 1348-1355.
- 487 20. Neale, P. A.; Escher, B. I.; Goss, K.-U.; Endo, S., Evaluating dissolved organic carbon–  
488 water partitioning using polyparameter linear free energy relationships: Implications for the  
489 fate of disinfection by-products. *Water Res.* **2012**, *46*, (11), 3637-3645.
- 490 21. Nguyen, T. H.; Goss, K.-U.; Ball, W. P., Polyparameter linear free energy relationships  
491 for estimating the equilibrium partition of organic compounds between water and the natural  
492 organic matter in soils and sediments. *Environ. Sci. Technol.* **2005**, *39*, (4), 913-924.
- 493 22. Endo, S.; Grathwohl, P.; Haderlein, S. B.; Schmidt, T. C., LFERs for soil organic carbon–  
494 water distribution coefficients ( $K_{oc}$ ) at environmentally relevant sorbate concentrations.  
495 *Environ. Sci. Technol.* **2009**, *43*, (9), 3094-3100.

496 23. Shih, Y.-h.; Gschwend, P. M., Evaluating Activated Carbon–Water Sorption Coefficients  
497 of Organic Compounds Using a Linear Solvation Energy Relationship Approach and Sorbate  
498 Chemical Activities. *Environ. Sci. Technol.* **2009**, *43*, (3), 851-857.